Engineering Failure Analysis 158 (2024) 107971

Contents lists available at ScienceDirect

Engineering Failure Analysis

journal homepage: www.elsevier.com/locate/engfailanal

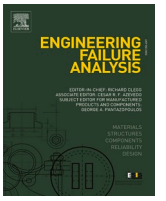

Re-evaluation of fatigue design curves for offshore wind monopile foundations using thick as-welded test specimens

Ali Mehmanparast [a,*], Amir Chahardehi [b], Feargal Brennan [a], Mark Manzocchi [b]

[a] Department of Naval Architecture, Ocean and Marine Engineering, University of Strathclyde, Glasgow G1 1XQ, United Kingdom
[b] Kent Energies, London SW1V 1PX, United Kingdom

ARTICLE INFO

Keywords:
Offshore wind turbine
Support structure
Monopile
Foundation design
Fatigue design

ABSTRACT

The dominant majority of existing offshore wind turbines are supported using monopile foundations which are fabricated by welding thick steel plates. In the current fatigue design recommendations for welded steel structures, which are commonly used in the design of monopile structures, the initial inverse slope of the S-N curve is fixed to −3. The historic rationales for this assumption are the ease of fatigue life calculations, the effect of long-range residual stresses that were not originally captured in the test data on thin welded specimens, and analogy with fatigue crack growth. While this introduces an unquantified level of conservatism to deterministic fatigue calculations, it was an acceptable (and wise) assumption when the S-N design curves were generated a few decades ago; however, current designs and assessments require more accurate calculations and the need to more confidently quantify the likelihoods attached to these evaluations. In the present study, it is argued that unlike large braced structures (e.g. jackets) in which long-range residual stresses may remain in place as fatigue cracks propagate, in circumferential welds of monopile structures the natural relaxation of residual stresses, in the absence of long-range residual stresses, must be accounted for by performing fatigue tests on thick welded samples. This paper presents a thorough analysis of the fatigue test results obtained from 50 mm thick as-welded samples with representative profiles of residual stresses that exist in monopiles. Basic and advanced statistical approaches were employed in the analysis and higher values of inverse slope were found using the large thickness test data. The results from this study are compared with the recommended fatigue design curves available in international standards. The outcomes from this research draw important observations concerning the need to employ an appropriate value of inverse slope in the design of monopile structures by excluding the conservative approach imposed by a fixed value of −3 which was originally implemented for braced structures with the assumption of large and long-range residual stresses.

1. Introduction

Offshore wind turbines (OWTs) are typically designed for an operational life of 20–30 years or even longer in more recent designs. These structures comprise three main parts which include the foundation, transition piece (TP) and tower. In recent years a number of TP-less OWT concepts have been developed by discarding the TP and installing the tower directly on top of the foundation. One of the most critical parts of the design process, particularly with provision for life-extension, is the selection and detailed engineering design

* Corresponding author.
E-mail address: ali.mehmanparast@strath.ac.uk (A. Mehmanparast).

https://doi.org/10.1016/j.engfailanal.2024.107971
Received 7 November 2023; Received in revised form 4 January 2024; Accepted 7 January 2024
Available online 9 January 2024

Nomenclature

A	The intercept in the general form of S-N curve equation
c	A statistical factor which depends on number of fatigue data points
k	Thickness exponent on fatigue strength
L	Specimen length
$\log a$	The intercept of the mean S-N curve with the log N axis
$\log \bar{a}$	The intercept of the design S-N curve with the log N axis
m	Inverse slope in the S-N curve
n	Number of fatigue data points
N	Number of cycles to failure
R	Load ratio
$s_{\log N}$(or σ)	Standard deviation with the log N axis
S (or $\Delta\sigma$)	Stress range in fatigue cycle
t	Specimen thickness
t_{ref}	Reference thickness
W	Specimen width
x_c	The confidence with respect to mean S-N data derived from a normal distribution
BM	Base metal
DFF	Design fatigue factor
HAZ	Heat affected zone
OWT	Offshore wind turbine
PDF	Probability density function
R&D	Research and development
SCF	Stress concentration factor
SD	Standard deviation
SLIC JIP	Structural Lifecycle Industry Collaboration Joint Industry Project
SMF	Stress modification factor
TP	Transition piece

of the OWT foundation. The fixed bottom foundation is the preferred solution for relatively shallow waters while the floating foundations are deployed in deeper waters. At the moment, the majority of deployed offshore wind farms in the UK and Europe are within shallow waters and the foundation type that has been dominantly used to support these OWTs is the monopile structure. OWT monopile foundations are fabricated by cold forming large thickness structural steel plates into cylindrical sections which are initially welded in longitudinal direction to produce cans and are subsequently welded circumferentially to manufacture the foundation at a desired length. Due to the large thickness of monopile structures, double V-groove or double J-groove multi-pass butt welding is conducted to join the metallic parts together.

Offshore wind monopiles are unique structures, and unlike wind turbine towers, ships and offshore jacket steel structures, they tend to be increasingly thick sections. This characteristic presents a number of challenges for fatigue resistance primarily associated with what is often referred to as the volumetric effect [1]. This phenomenon in a simple way can be described as the greater the volume of material the greater the likelihood of defects. The fatigue life of welded structures is heavily influenced by the presence of near surface defects and stress concentration at the weld toes in the case of as-welded joints. The thicker sections typically have relatively lower fatigue lives than thinner equivalents due to the higher constraint level and large extent of damaging residual stresses during a longer period of crack growth. Moreover, once the fatigue crack initiates at the weld toe region the crack propagation behaviour can be influenced by the geometric stress concentration factor (SCF) from a larger weld cap size and the variation in mechanical properties along the through-thickness direction.

Fatigue design guidance and standards for offshore welded structures have developed incrementally over the decades, and for monopile structures they were adapted from the standards originally designed for thinner Oil & Gas and ship structures. Indeed, it is well-known in the offshore wind sector that there are substantial uncertainties around the level of conservatism involved in the existing fatigue design curves for large-scale OWT monopile application. Today the most common standard and guidance for the design of offshore wind monopiles is provided by DNV [2,3], with a number of updates throughout the years to include learnings from in-service experience of the industry. DNV publishes its standards and recommended practice documents on the public domain and is explicit in stating [4]: "*DNV is not responsible for the consequences arising from any use of these documents*". This simply implies that any use of the fatigue design recommendations in DNV standard is at the users' sole risk and DNV does not accept any liability or responsibility for loss or damages resulting from any such use. An example of this was part of a UK Supreme Court judgement (August 2017) [5] where the relevant DNV guidance was incorrect (this was revised subsequently in the following update of the standard) and the Supreme Court found the responsibility for the error was with the designer, rather than the standardisation body. The learning from this case is that it is up to the user to evaluate whether or not an operation is fit-for-purpose. Whereas the operator will frequently follow practices and procedures detailed in DNV standards and other certification documents, it will often be supplemented by other expert advice. The

Supreme Court ruling makes it clear that an owner or designer cannot abdicate responsibility or transfer this to a standard/certification body.

The laboratory test data sets, based on which the current fatigue design curves specified in international standards such as DNV-RP-C203 [3], were taken from experiments on relatively thin samples representing the dimensions of bridge structural components, offshore Oil & Gas structures and pipelines rather than much thicker OWT monopiles. Although an empirical equation is provided in DNV-RP-C203 to estimate the fatigue life for thicker structures, the upper bound limit for application of the recommended equation is not specified. Moreover, the existing design curves are generated using relatively simple statistical data analysis approaches. In order to address the essential need for developing a deeper understanding of the fatigue design and life analysis for OWT monopiles, this paper re-evaluates the design curves for as-welded offshore wind monopile structures by applying advanced statistical analysis methods on large thickness test data from a recent round robin test programme and compares the obtained results with the traditional linear regression analysis fits and the recommendations specified in international standards. The observations from this study do not only provide an insight into the fatigue design for thick OWT monopile foundations but also present an innovative data analysis approach to develop reliable fatigue design curves from small-to-medium number of tests on thick specimens.

2. A summary of the recommended practice for fatigue design of welded structures

There are a number of international standards which describe the recommended practice for fatigue design of welded structures. These standards include “DNV-RP-C203: Fatigue design of offshore steel structures” [3], “API Recommended Practice 2A-WSD: Planning, designing, and constructing fixed offshore platforms—working stress design” [6], “BS 7608: Guide to fatigue design and assessment of steel products” [7] and “Eurocode 3: Design of steel structures” [8]. In each of these standards recommended fatigue design curves are provided for different classifications of welds including the transverse load carrying butt weld (as-welded), which is often referred to as D curve. In DNV-RP-C203 and BS 7608 the recommended fatigue design curves are described for three different environmental conditions of air, seawater with cathodic protection and seawater with free-corrosion, whereas in Eurocode 3 the fatigue design curves are specified only for the air environment. It is worth noting that BS 7608 explicitly states that its recommendations are not applicable to fixed offshore structures. In offshore wind industry, the recommendations and guidelines described in DNV-RP-C203 are widely used for the design of OWT monopile foundations. The majority of the monopiles are designed and fabricated based on the as-welded condition described by D curve in DNV-RP-C203. This is mainly due to time and cost saving by targeting a larger thickness to achieve a desired fatigue life in the presence of stress risers at the weld toes as opposed to allocating extra time and cost for grinding the weld toes upon completion of the welding process.

The recommended design curves specified in international standards were originally generated by performing uniaxial fatigue tests on welded plates under cyclic loading condition. Using this approach, repeated number of fatigue tests are performed at various stress levels and the obtained results are reported by plotting the stress range S in MPa, against the number of cycles to failure N. These graphs, which are the basis of fatigue design, are known as the S-N curves that appear as straight lines in log–log axes. Using a population of experimental fatigue data points generated for a given surface condition, a mean fit is made to the data by conducting a regression analysis and the inherent scatter in the data set is captured by evaluating the standard deviation (SD) and subsequently plotting “mean + 2SD” and “mean-2SD” curves to obtain the upper bound (i.e. best case) and lower bound (i.e. worst case or ‘design curve’), respectively, in the S-N data analysis (see Fig. 1). The “mean-2SD” from the statistical analysis accounts for the necessary conservatism in the design process by considering the material variability and weld quality, and therefore is employed in the design of OWT welded structures in conjunction with design fatigue factor (DFF) to achieve a desired target probability of failure.

The S-N design curves in general form can be defined using the following equation [3]:

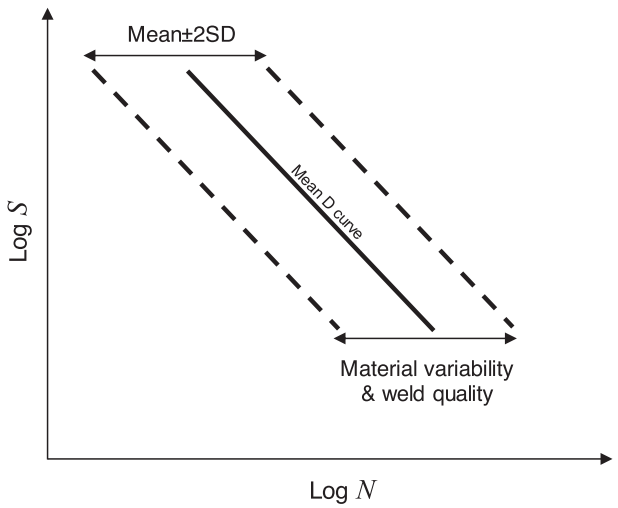

Fig. 1. Schematic demonstration of mean and mean ± 2SD fatigue curves for as-welded condition.

$$\log N = \log\bar{a} + m\log S \tag{1}$$

where S (or $\Delta\sigma$) is the stress range in MPa, N is the number of cycles to failure, m is the inverse slope in the S-N curve which is always a negative number (hence why the DNV standard presents it as -m), and $\log\bar{a}$ is the intercept of the design S-N curve with the log N axis.

The correlation between the intercepts of the mean and mean-2SD curves can be described by:

$$\log\bar{a} = \log a - 2s_{\log N} \tag{2}$$

where $\log a$ is the intercept of the mean S-N curve and $s_{\log N}$ is the standard deviation with the log N axis. In DNV-RP-C203 [3] only the design curves are provided and the mean curves can be estimated following the recommendation to take $s_{\log N} = 0.2$ for butt-welded structures, whereas in BS 7608 [7] both mean and design curves are provided and specific values of $s_{\log N}$ are presented for different classes of weld.

As explained earlier, it is known that the fatigue life of a welded structure depends on the plate thickness. Therefore, an empirical modification factor is provided in DNV-RP-C203 [3] to estimate the S-N curve for welded structures with various thicknesses using the following relationship:

$$\log N = \log\bar{a} + m\log\left(S\left(\frac{t}{t_{ref}}\right)^{k}\right) \tag{3}$$

where t_{ref} is the reference thickness equal to 25 mm for welded connections other than simple tubular joints, k is the thickness exponent on fatigue strength, the values of which can be found in [3], and t is the thickness through which a crack will most likely grow. It is recommended in [3] to take t as t_{ref} for thicknesses of smaller than t_{ref}. A similar thickness modification factor can be also found in BS 7608 [7]. It is worth noting that there is no upper limit specified in standards for validity of the thickness correction factor which may introduce some degree of uncertainty when the S-N curves are estimated for welded structures with thickness values of much larger than 25 mm. The S-N fatigue design curve for the as-welded condition (i.e. D curve) in air based on DNV-RP-C203 recommendations is shown in Fig. 2 for the reference thickness value of 25 mm and compared with the larger thickness value of 50 mm. As seen in Fig. 2 and Eq. (3), for a given value of stress range an increase in the thickness results in a reduction in fatigue life. In case of 50 mm thickness, the ratio of calculated design lives for the first slope is 0.66, and 0.5 for the second slope part of the curve, leading to a reduction of 34–50 % in calculated fatigue life compared to the reference thickness of 25 mm.

3. SLIC project

3.1. Motivation for fatigue testing on large thickness samples

The recommended fatigue design curves in international standards were originally derived a few decades ago from constant amplitude tests (mostly $N \leq 10^7$ cycles) where the majority of the specimens had much thinner sections than current OWT monopile structures. Conducting a fatigue test programme on thinner specimens compared to the actual structure poses two fundamental problems for fatigue design of welded joints: firstly, the structure's constraint level (which can lead to long-range residual stress) is not replicated in the test specimens, and secondly in thicker specimens the crack experiences large extents of residual stresses during a longer period of its growth [9]. Even if the fatigue test specimens are extracted from large-scale welded structures, residual stresses are known to be redistributed during the cutting process, therefore extra attention must be paid in design and fabrication of welded specimens which would represent the residual stress state in large-scale welded structures.

While the thickness modification factor in DNV-RP-C203 standard (see Eq. (3)) aims to capture the thickness effect, it doesn't

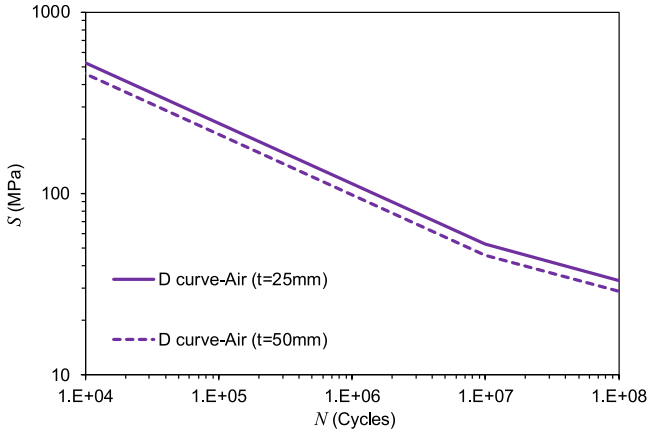

Fig. 2. Comparison of S-N design curves for as-welded condition (D curve) in air for the thickness values of 25 and 50 mm.

account for the change in residual stresses from small-scale samples to large-scale welded structures. A recommendation that has been proposed in DNV-RP-C203 to compensate for the reduced level residual stresses in small-scale welded specimens, compared to full scale structure, is to perform fatigue tests at a high load ratio of around $R = 0.5$, where R is the ratio of minimum load/stress to maximum load/stress in a fatigue cycle. This is to capture effect of any long-range residual stresses that are present in the structure (due to git up, constraint, etc). This means that while DNV-RP-C203 provides conservative recommendations applicable to a wide range of welded structures, for the case of OWT monopiles a high R-ratio replicates a high level of tensile residual stress in the small-scale specimen during the entire test period. While the long-range residual stresses in monopile girth welds are not fully determined, it is unlikely that the same level of constraint exists as other braced structures such as jackets. Additionally, in the absence of high magnitude structural residual stresses, in reality the weld could lose part of its residual stresses at the hot spots over time when subjected to cyclic loading conditions. For experimental investigations available on redistribution and relaxation of residual stresses in welds under cyclic loading see for example [10–12].

Due to the gaps in the knowledge identified above and to enhance the best practice for the fatigue design of OWT monopiles, the Structural Lifecycle Industry Collaboration Joint Industry Project (SLIC JIP) was created. Significant outputs from the programme included material characterisation and fracture mechanics data [13–15] representing a very important body of information for life assessment of monopile structures. The focus of the present study is to re-analyse the S-N fatigue data on thick as-welded samples obtained from the SLIC JIP [16]. A summary of the SLIC S-N test details is presented next and the evaluation of the test results and comparison with the standard design curves is presented in the following sections.

3.2. Experimental details

The uniaxial fatigue tests in the SLIC project were conducted on large-scale dog-bone shaped specimens with the thickness of $t = 50$ mm, width of $W = 100$ mm and total length $L = 1.5$ m. The experimental investigations in the SLIC project were conducted by doubling the thickness of the fatigue test specimens, compared to the reference thickness of 25 mm specified in DNV-RP-C203 standard, to evaluate the fatigue life in OWT monopile circumferential welds with the thickness values of much higher than 25 mm. The material used in the S-N fatigue round robin test programme was S355ML structural steel which is widely used in fabrication of OWT structures including monopiles. During the fabrication phase, double V-grooved steel plates with 50 mm thickness were multi pass butt welded using the welding procedure employed in the manufacture of OWT monopile structures. The misalignment angle and welding defects were carefully evaluated post-welding to only consider the welded plates which were acceptable by the current best practice in the offshore wind industry. Large thickness dog-bone specimens were extracted from the welded plates with the loading axis perpendicular to the welding direction and without grinding the weld toe (i.e. as-welded condition). Each specimen was strain gauged on two opposite sides to capture the misalignment and consider it in the analysis. Due to the large cross-sectional area of the specimens, the tests were conducted using 2.5 MN machines to reach the target load values during the tests. All tests were performed in air under constant amplitude cyclic loading condition with load control mode and the load ratio of $R = 0.1$. More details about the specimen design, test set-up and loading condition can be found in [16].

Due to the dependence of the design curve on SD (see Eq. (2)), it is quite important to perform sufficient number of experiments to capture the material variability and welding quality which would impact the inherent scatter in the data. To achieve a sufficiently high confidence level in statistical analysis of the fatigue data it would be ideal to perform a very large number of tests; however, for large-scale fatigue testing this would be too costly and impractical hence the number of specimens must be carefully selected. In the SLIC project 31 tests were conducted in total on as-welded specimens. 29 of these tests were continued until failure (i.e. full width crack formation) whereas the remining 2 tests were suspended without any sign of crack initiation and reported as run outs. It is worth noting that a few of the data points lie beyond 2 million cycles, and these points may be approaching the endurance limit or require special treatment considering the possibility of a change of slope (although the evidence for this is not strong for constant amplitude loading). It was decided to ignore this possibility for the current investigation.

The number of uniaxial fatigue tests in the SLIC project satisfies the recommendations provided in ASTM E739-10 [17] to conduct 6—12 tests for research and development (R&D) studies, and also 12—24 tests for design allowance. Similar recommendations can be found in BS EN ISO12107 [18].

4. Basic and advanced statistical approaches for fatigue data analysis

4.1. Basic statistical analysis methodology

The linear regression model for a basic statistical analysis on a population of fatigue data points can be described as:

$$\log(N_i) = A + m\log(S_i) + \epsilon_i \tag{4}$$

where N_i and S_i are the increments of number of cycles to failure and stress range values, respectively, taken from the fatigue data set, A is the intercept, m is the inverse slope in the S-N curve which always appears as a negative number, and ϵ_i are increments of independent normally distributed residuals with standard deviation $s_{\log N}$. For a given fatigue data set, the parameters A, m and $s_{\log N}$ can be estimated by performing a linear regression analysis. This is the basic statistical analysis model that has been historically employed in derivation of fatigue design curves in international standards from the population of experimental data points obtained from laboratory testing.

4.2. Advanced statistical analysis methodology

4.2.1. Bayes theorem

In general, if we have a random model with exchangeable variables $\mathbf{X}$ and distribution parameter θ, the joint probability density function (PDF) is given by:

$$f_{\mathbf{X},\theta} = f_{\mathbf{X}|\boldsymbol{\theta}} f_{\boldsymbol{\theta}} = f_{\boldsymbol{\theta}} \prod_i f_{X_i|\boldsymbol{\theta}} \tag{5}$$

Given data $\mathbf{X_{data}}$, the posterior distribution of θ conditional on the data is given by:

$$f_{\theta|\mathbf{X_{data}}} = \frac{f_{\boldsymbol{\theta}} \prod_i f_{X_i|\boldsymbol{\theta}}}{f_{\mathbf{X_{data}}}} = \frac{f_{\mathbf{X_{data}},\theta}}{f_{\mathbf{X_{data}}}} \tag{6}$$

Considering that the denominator $f_{\mathbf{X_{data}}}$ is a constant for given data set, the posterior distribution can be expressed as:

$$f_{\theta|\mathbf{X_{data}}} \propto f_{\boldsymbol{\theta}} \prod_i f_{X_{data\,i}|\boldsymbol{\theta}} \tag{7}$$

This is defined to a proportionality constant, and samples can be taken using Markov Chain Monte Carlo methods.

4.2.2. Bayesian regression model

By rearranging the linear regression model in Eq. (4), the residuals can be written as:

$$\epsilon_i = \log(N_i) - (A + m log(S_i)) \sim N(0, s_{\log N}) \tag{8}$$

Hence the joint PDF of the data and parameters can be described as:

$$f_{A,m,s_{\log N},\epsilon} = f_A f_m f_{s_{\log N}} f_{\epsilon|A,m,s_{\log N}} \tag{9}$$

$$f_{\epsilon|A,m,s_{\log N}} = \phi\left(\epsilon, 0, s_{\log N}\mathbf{I}\right) \tag{10}$$

$$f_{A,m,s_{\log N},\epsilon} = f_A f_m f_{s_{\log N}} \prod_i \phi\left(\epsilon_i, 0, s_{\log N}\right) \tag{11}$$

The analysis of the test data gives $\epsilon_i = \log(N_i) - (A + m log(S_i))$. The conditional distribution of the parameters A, m, and $s_{\log N}$ is then given, by Bayes rule, as being proportional to:

$$f_{A,m,s_{\log N}|\epsilon} \propto f_A f_m f_{s_{\log N}} \prod_i \phi\left(\log(N_i) - (A + m log(S_i)), 0, s_{\log N}\right) \tag{12}$$

where f denotes PDF and $\phi\left(x, \mu, s_{\log N}\right)$ denotes normal PDF.

4.2.3. Censoring terminated test data

In order to add a feature to realistically account for the tests which were terminated before failure (also referred to as run outs or suspended tests), a new function can be defined in the analysis to include the censored data. In the case of terminated tests, the actual number of cycles to failure can be described by:

$$N_i > N_{t_i} \tag{13}$$

where N_i is the actual number of cycles to failure for a suspended fatigue test in a data set and N_{t_i} is number of cycles at which the test was terminated. Eq. (13) shows that the actual number of cycles to failure is greater than the terminated number of cycles.

Combining Eq. (4) and Eq. (13), the residuals for the terminated test data, ϵ_t, can be described as:

$$\epsilon_i > \log(N_{ti}) - (A + m log(S_i)) = \epsilon_t \tag{14}$$

The posterior distribution (for a single test – multiple tests are a product) is then described as:

$$\begin{aligned} f_{A,m,s_{\log N}|\epsilon_i > \epsilon_{t_i}} &= f_A f_m f_{s_{\log N}} \int_{\epsilon_t}^{\infty} \phi\left(\epsilon, 0, s_{\log N}\right) d\epsilon = f_A f_m f_{s_{\log N}} \int_{\log(N_{ti}) - (A + m log(S_i))}^{\infty} \phi\left(\epsilon, 0, s_{\log N}\right) d\epsilon \\ &= f_A f_m f_{s_{\log N}} \left(1 - \Phi\left(\log(N_{ti}) - (A + m log(S_i)), 0, s_{\log N}\right)\right) \end{aligned} \tag{15}$$

Splitting data into completed tests (with subscript c) and terminated tests (with subscript t), the posterior distribution is then defined as:

$$f_{A,m,s_{\log N}|\epsilon=0} \propto f_A f_m f_{s_{\log N}} \prod_{i_c} \phi\left(\log\left(N_{c i_c}\right) - \left(A + m log\left(S_{c i_c}\right)\right), 0, s_{\log N}\right) \prod_{i_t} \left(1 - \Phi\left(\log\left(N_{t i_t}\right) - \left(A + m log\left(S_{t i_t}\right)\right), 0, s_{\log N}\right)\right) \tag{16}$$

4.2.4. Sampling of posterior distributions

In this study, sampling from the posterior distribution was performed using the STAN Hamiltonian Markov chain Monte Carlo sampler implemented in the RStan software package. The prior distributions are intended to be non-information; for A normal with mean 0 and standard deviation 1000, for m normal with zero mean and standard deviation 100, and for $s_{\log N}$ uniform between 0 and 100. Sampling was carried out from four chains, each with 5,000 samples and a burn-in of 5,000 samples, with a total of 20,000 samples, using the Hamiltonian Markov Chain Monte Carlo sampling algorithm NUTS implemented in RStan software.

5. Fatigue analysis of thick as-welded test data

5.1. Linear regression analysis

The fatigue test data from the SLIC project [16] (see Appendix A) was employed in this study and the linear regression analysis was initially conducted to evaluate the mean and mean±2SD curves. The analysis was performed by considering the misalignment effect, captured using the strain gauge data, on the actual stress range values. The linear regression analysis was carried out on completed test data without considering the suspended data points (run outs) and the results are shown in Fig. 3. Also included in Fig. 3 is the repeated linear regression analysis using the fixed inverse slope of $m = -3$ which is the recommended value for design of as-welded structures in DNV-RP-C203 [3] for $N \leq 10^7$ cycles. The values of inverse slope m and intercept A obtained from the linear regression analysis using variable (i.e. unfixed) and fixed inverse slope assumptions are summarised in Table 1. Also included in Table 1 are the values of SD for each scenario. It can be observed in Fig. 3 and Table 1 that the value of the inverse slope obtained from the linear regression analysis on the completed SLIC test data (i.e. by excluding the run outs) is $m = -3.37$. Moreover, it can be seen in Table 1 that by fixing the inverse slope of the S-N curve to $m = -3$, the value of intercept decreases. Furthermore, it can be seen in Table 1 that the standard deviation for the completed test data is 0.21, which is very close to the general assumption of 0.2 in DNV-RP-C203 for welded joints with a random misalignment [3].

Comparing the regression fits obtained from the variable inverse slope to the $m = -3$ assumption in Fig. 3 it can be seen that fixing the inverse slope following the guidelines provided in international standards such as DNV-RP-C203 [3], BS 7608 [7] and Eurocode 3 [8] can result in un-conservatism in the high stress (i.e. low cycle) region and over-conservatism in the low stress (i.e. high cycle) region specially if the curves are extrapolated to $N = 10^7$ cycles, which is the switch over point for the inverse slope of -3 according to DNV-RP-C203 [3]. The fatigue design life calculation using the linear regression fits presented in Table 1 shows that at $N = 10^7$ the number of cycles to failure obtained from the variable inverse slope would be 1.6 times higher than that obtained from the fixed inverse slope of $m = -3$ at the same stress range level. This indicates that the level of conservatism in fatigue life estimation of monopile welded structures in the high cycle region may significantly reduce by considering a higher value of m obtained from the SLIC test data which may be supported with additional large-scale tests in the future. This observation highlights the fact that while the fixed slope of -3 specified in DNV-RP-C203 for $N < 10^7$ cycles might be an acceptable assumption for thinner offshore welded structures specially in the

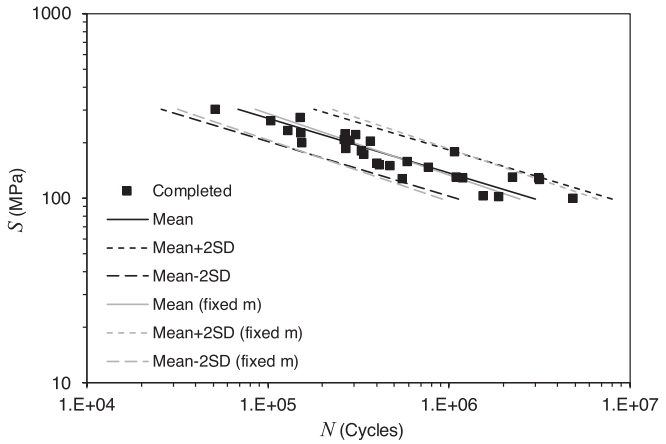

Fig. 3. Mean and mean ± 2SD fits from linear regression analysis on the SLIC data using variable and fixed inverse slope assumptions by excluding run outs.

Table 1
Inverse slope and intercept values for the mean and mean-2SD curves obtained from linear regression analysis on completed SLIC data points.

Variable/fixed inverse slope	Mean		Mean-2SD		$s_{\log N}$
	$\log a$	m	$\log \bar{a}$	m	
Variable	13.210	−3.37	12.786	−3.37	0.21
Fixed	12.380	−3.00	11.953	−3.00	0.21

presence of long-range residual stresses (i.e. in braced structures such as jackets), extending the application of this fixed slope to much thicker OWT monopile structures can result in under-prediction of the fatigue damage during the pile driving process, which takes place under very high stress values, and over-conservative designs for the operational phase of monopiles with low stresses and high number of cycles.

5.2. Bayesian regression analysis

The results from the Bayesian regression on the SLIC test data using variable (i.e. unfixed) and fixed inverse slope are presented in Fig. 4 (a) and (b) for the analysis with the censored data (including run outs with the fatigue life described using Eq. (13)) and uncensored data (excluding run outs), respectively, and the values of intercept and inverse slope for mean and mean-2SD curves are summarised in Table 2. Further results from the Bayesian regression analysis (including the histograms of Markov chain Monte Carlo samples of regression parameters A, m and $s_{\log N}$, which is referred to as σ, and the properties of the 2.5th, 25th, 50th, 75th and 97.5th percentiles) by including and excluding the suspended test data points can be found in Appendix B. As seen in Fig. 4 and Table 2, the analysis of the test data using Bayesian regression model shows that for both scenarios of censored and uncensored data the inverse slope has a magnitude of larger than −3. Also seen in Table 2 is that the increase in the magnitude of m, compared to the fixed m of −3, results in a significant reduction in the intercept value of A. The obtained results from the Bayesian regression analysis in Fig. 4 show that similar to the linear regression analysis results in Fig. 3, the fixed inverse slope of m = -3 leads to unconservative and over-conservative fatigue design curves in the high stress and low stress regions, respectively. The fatigue design life calculation using the Bayesian regression fits presented in Table 2 shows that at $N = 10^7$ the number of cycles to failure obtained from the variable inverse slope would be 1.9 and 1.6 times higher than that obtained from the fixed inverse slope of m = -3 at the same stress range level for the censored and uncensored test data, respectively.

Moreover, it can be observed in Table 2 that, excluding the run outs in Bayesian regression analysis results in a lower value of $s_{\log N}$. Comparing Table 1 and Table 2 it can be seen that the value of $s_{\log N}$ obtained from the Bayesian regression analysis by excluding the run

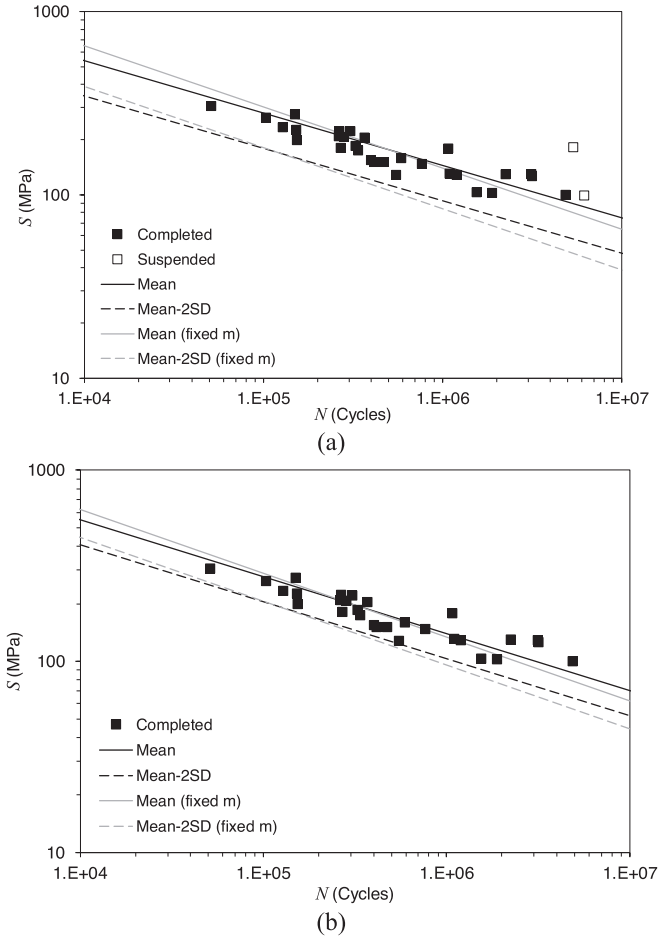

Fig. 4. Mean and mean-2SD fits from Bayesian regression analysis on the SLIC data using variable and fixed inverse slope assumptions by (a) including the suspended test data points with the fatigue life described using Eq. (13), (b) excluding run outs.

Table 2
Inverse slope and intercept for the mean and mean-2SD curves obtained from Bayesian regression analysis on the SLIC data.

Censored/Uncensored	Variable/fixed inverse slope	Mean		Mean-2SD		$s_{\log N}$
		$\log a$	m	$\log \bar{a}$	m	
Censored	Variable	13.563	−3.50	12.888	−3.50	0.34
Censored	Fixed	12.439	−3.00	11.773	−3.00	0.34
Uncensored	Variable	13.206	−3.36	12.765	−3.36	0.22
Uncensored	Fixed	12.380	−3.00	11.940	−3.00	0.22

outs is slightly higher than the linear regression analysis. Moreover, it can be seen in Table 2 that when the Bayesian regression model in employed in the analysis of the uncensored data, by excluding the suspended test data points, the values of the inverse slope and intercept are almost identical to the ones obtained from the linear regression analysis in Table 1. Also seen in Table 2 is that for the case of censored data, by including the suspended test data points with the fatigue life described using Eq. (13), the magnitude of the inverse slope m and intercept A have been found to be slightly larger than the uncensored results using the variable (i.e. unfixed) inverse slope assumption. The results from both regression models show that the magnitudes of inverse slope obtained from large thickness SLIC test data are larger than the fixed value of m = -3 for $N \leq 10^7$ cycles specified in DNV-RP-C203. While the inverse slope obtained from the linear regression is found to be −3.37, the solutions from Bayesian regression analysis are found to be in a wider range of $-3.5 \leq m \leq$ -3.36.

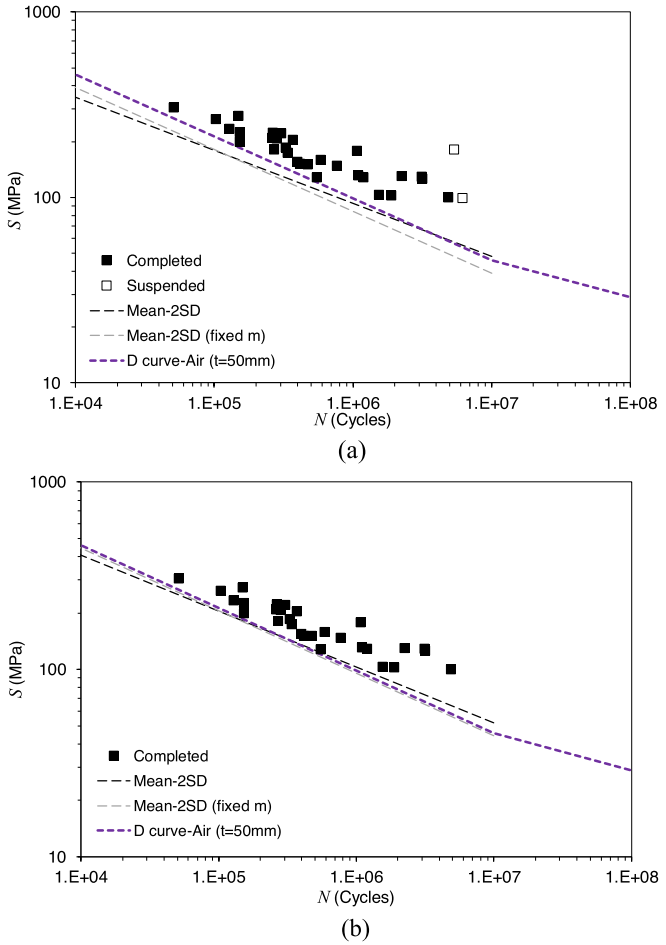

Fig. 5. Comparison of the fatigue design curve with mean-2SD fits from Bayesian regression analysis on the SLIC data using variable and fixed inverse slope assumptions by (a) including the suspended test data points with the fatigue life described using Eq. (13), (b) excluding run outs.

6. Comparison of the regression analysis results with the standard design curve

6.1. Comparison of Bayesian regression lines with DNV design curve

The mean-2SD curves obtained from Bayesian regression analysis on the SLIC data using variable (i.e. unfixed) and fixed inverse slope assumptions are compared with the thickness corrected ($t = 50$ mm) D curve estimated by Eq. (3) in Fig. 5(a) and (b) using the censored (i.e. including the suspended test data points with the fatigue life described using Eq. (13)) and uncensored (i.e. excluding run outs) data, respectively. As seen in Fig. 5(a), when the run outs are considered in the analysis the mean-2SD curves based on variable and fixed inverse slopes fall behind the thickness corrected D curve with the variable inverse slop curve converging towards the D curve in the high cycle region. However, Fig. 5(b) shows that the underprediction of fatigue life using the thickness corrected D curve is largely improved when the run outs are excluded from the analysis. It can be observed in Fig. 5(b) that mean-2SD curve obtained from the Bayesian regression using variable inverse slope falls behind and ahead of the thickness corrected D curve at high stresses and low stresses, respectively. This means that if variable inverse slope is considered in the analysis, the thickness corrected D curve would underpredict the fatigue life in high stress region and overpredict fatigue life in the low stress region close to N of 10^7 cycles. Also seen in Fig. 5(b) is that by fixing the inverse slope to $m = -3$ in the Bayesian regression analysis, the obtained mean-2SD curve falls close to, and just below, the thickness corrected D curve. The general observation in Fig. 5 is that the consideration of run outs and also changing the inverse slope to a fixed value would significantly influence the position of the mean-2SD curves from Bayesian regression analysis with respect to the thickness corrected design curve.

6.2. Comparison of linear regression lines from completed tests with the design curves following DNV guidelines

There are two approaches for derivation of revised fatigue design curves that are explained in DNV-RP-C203 [3]. Using the first approach pure statistical analysis is conducted by applying some degree of engineering judgment to account for the number of completed tests and population size. In the second approach, a limited number of completed tests can be conducted to validate the use of a particular design S-N class. Both of these approaches, which consider only the fatigue tests completed to failure by excluding the run outs, are briefly explained next and the analysed SLIC results are presented based on each approach.

6.2.1. Analysis of the SLIC data using the statistical approach

According to all international standards including DNV-RP-C203 [3] and BS 7608 [7], the probability of survival for S-N design curves must be 97.7 % whilst the probability of survival for the mean curve is 50 %. As shown in Eq. (2), when a large number of data points is available in an experimental data set, the S-N design curve can be generated by deducting two SD from the mean curve assuming that the data follow a Gaussian distribution on a logarithmic scale [19]. While mean-2SD provides a reliable estimate of the design curve for a data set with large number of points, the lack of sufficient number of data points would introduce uncertainly in this estimate. This is usually the case when limited number of data points are available from large-scale welded samples which are difficult and expensive to manufacture and test.

According to DNV-RP-C203 standard [3], the range of confidence level required to estimate the S-N design curve is between 75 % and 95 %. Based on these guidelines, for n observations of the number of cycles to failure, N, obtained from experiments conducted at various stress ranges, S, the S-N design curves can be estimated using Eq. (1) by considering an acceptable range of confidence level which can be described by:

$$\log\bar{a} = \log a - cs_{\log N} \tag{17}$$

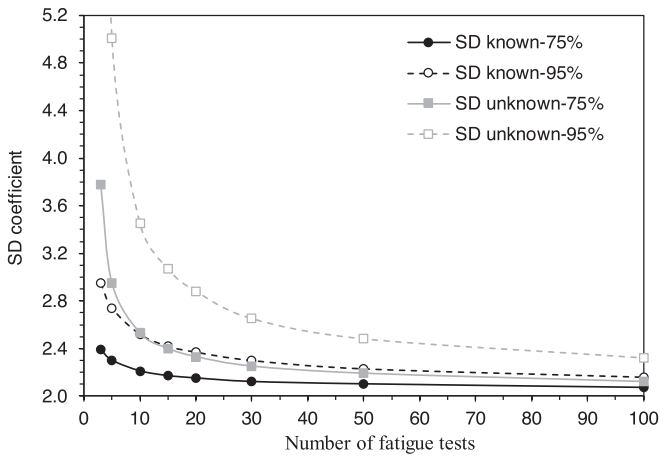

Fig. 6. The variation of statistical factor based on 75% and 95% confidence levels and unknown/known SD, taken from [3].

where log$a$ is the intercept of the mean curve for n test data with the log N axis, $s_{\log N}$ is the standard deviation of the n test data with the log N axis, and c is a statistical factor that depends on number of fatigue data points, n. The values of c parameter for different number of tests can be found in Fig. 6 for two scenarios of known and unknown SD. As seen in Fig. 6, with a decrease in the number of fatigue data points the SD coefficient, c, exponentially increases to maintain 75 %—95 % confidence level. Also observed in this figure is that for a given confidence level, regardless of the number of tests the values of c are always higher when the SD is unknown compared to the known SD case. Finally seen in Fig. 6 is that for both known and unknown SD cases, the value of c is always higher for 95 % confidence level compared to 75 % confidence level, as expected. The values for the c factor presented in Fig. 6 are derived for independent variables by keeping the slope of the S-N curve constant when the regression analysis is carried out. In the case of dependent variables, where log N is dependent on log S, the values of c factor presented in Fig. 6 should be taken as approximate solutions and no extrapolation should be made beyond the stress ranges captured by the experimental data set.

The linear regression results on the SLIC data set (see Table 1) were further analysed following the procedure described above and the results are shown in Fig. 7(a) and (b) based on variable (i.e. unfixed) and fixed inverse slope assumptions, respectively. The results presented in Fig. 7 are based on independent variables, by taking the inverse slope as a constant which is obtained from the mean curve. Moreover, as instructed by DNV-RP-C203 [3] only the data points from the test which were conducted to failure have been implemented in the analysis and the run outs have been excluded.

The results in Fig. 7 show that using the statistical approach for both variable and fixed inverse slope assumptions, the values of c factor are found to be slightly over 2 for different confidence levels of 75 % and 95 % and also known and unknown SD scenarios. This means that the design curves based on each of these assumptions which result in "mean-cSD" curves are slightly shifted below the "mean-2SD" curve. While the design curves based on all of these assumptions fall close to each other in log–log axes, the most and least conservative lines are obtained from 95 % confidence with unknown SD and 75 % confidence level with known SD assumptions, respectively. The results from the statistical analysis are compared with the design D curve taken from DNV-RP-C203 [3] and thickness corrected for $t = 50$ mm (see Eq. (3)) for direct comparison with the SLIC results. It can be seen in Fig. 7(a) that using the variable inverse slope of $m = -3.37$, the thickness corrected design D curve is found to be unconservative for the high stress fatigue lives whereas

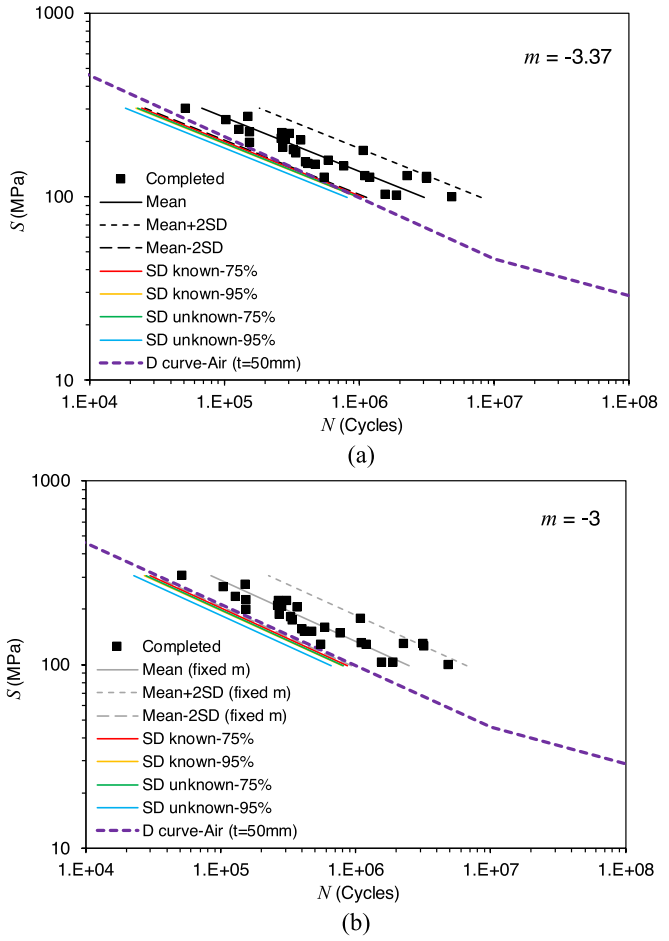

Fig. 7. Analysis of the linear regression results from the SLIC data using DNV's statistical approach based on two different confidence levels and unknown/known SD (a) variable inverse slope, and (b) fixed inverse slope.

in the low stress region the predicted trends show convergence towards the thickness corrected D curve. Using the fixed inverse slope of $m = -3$ in Fig. 7(b) it can be seen that the thickness corrected D curve is found to be unconservative compared to "mean-2SD" curve from the linear regression analysis as well as the obtained curves based on DNV's statistical approach for 75 % and 95 % confidence levels with unknown and known SD. The results in Fig. 7 show the inverse slope value can significantly influence the fatigue design of monopiles and while the fixed inverse slope of -3 may introduce a level of conservatism in the revised design curves obtained following the statistical approach specified in DNV-RP-C203, the variable slope assumption can lead to conservative revised curves, compared to thickness corrected D curve, only in the high stress region.

6.2.2. *Modification of the D curve using the SLIC data*

As mentioned in DNV-RP-C203 standard [3], large-scale testing on welded samples, which are manufactured by replicating the fabrication process in the actual structure, is quite challenging and costly; therefore, it is recommended to put as much emphasis as possible on such test results even if only one large-scale test representing the real-life structure is performed. This is particularly important due to the fact that large-scale welded samples which are capable of mimicking the structural constraint level can better describe the fatigue response of the real-life structure. Hence DNV-RP-C203 explicitly advises the standard users to thoroughly consider the fatigue response of large-scale welded samples which could add significant confidence to the design of real-life structures compared to small-scale test specimens. As such, an alternative approach has been detailed in DNV-RP-C203 standard which facilitates the use of existing design curves which are subsequently modified in accordance with the results obtained from a limited number of new large-scale tests.

The main assumptions in this approach are to: (a) take the existing S-N curves available in DNV-RP-C203 standard with suggested values of SD, and (b) consider the results from the tests which were continued to failure (i.e. full width crack formation) and exclude the run outs. Since this approach is based on a limited number of new data points, the slope of the new mean curve is assumed to be the same as the particular class of S-N design curve chosen from the standard. Using this approach, a mean S-N curve based on the new test data can be defined as:

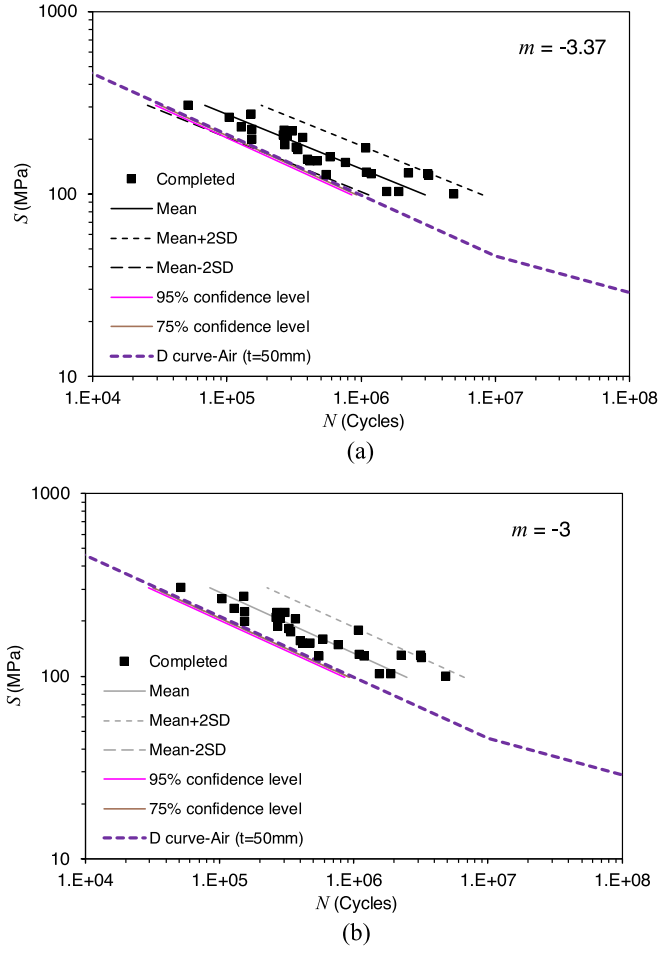

Fig. 8. Development of revised design curves using D curve and large thickness SLIC data based on (a) variable inverse slope, and (b) fixed inverse slope.

$$\log N = \log a + m\log(S \times \mathrm{SMF}) + \frac{x_c}{\sqrt{n}} s_{\log N} \quad (18)$$

where N is the number of cycles to failure, $\log a$ is the intercept of the considered mean standard S-N curve, m is the inverse slope of the standard S-N curve (which is always a negative number hence why the DNV standard presents it as -m), S is the stress range, SMF is the stress modification factor the calculation of which is detailed in DNV-RP-C203 standard, n is the number of test samples, x_c is the confidence with respect to mean S-N data derived from a normal distribution (which is 0.674 for 75 % confidence level and 1.645 for 95 % confidence level) and $s_{\log N}$ is the SD with the log N axis.

The linear regression results on the completed tests (i.e. excluding the run outs) from the SLIC project (see Table 1) were further analysed following the procedure described above and the results are shown in Fig. 8(a) and (b) based on variable (i.e. unfixed) and fixed inverse slope assumptions, respectively. From this analysis, the SMF value of 1.05 and 1.02 were obtained for the confidence levels of 95 % and 75 %, respectively. While these values are both very close to 1, slightly larger value of SMF has been obtained for 95 % confidence level compared to 75 % confidence level in the analysis.

The revised design S-N curves based on 95 % and 75 % confidence level have been presented in Fig. 8 and compared with the thickness corrected D curve with $t = 50$ mm and also the mean and mean $\pm$ 2SD curves from the linear regression analysis on the SLIC data. The results show that by considering the SLIC data, the D design curve in DNV-RP-C203 can be revised and made more accurate for OWT monopiles by introducing a slight shift of the S-N curve to the left. It can be seen in Fig. 8(a) that for the case of variable inverse slope, the revised D curves with both 95 % and 75 % confidence levels are found to be unconservative and conservative for high and low stress values, respectively, compared to mean-2SD curve from the linear regression analysis.

The comparison of the obtained results with the linear regression fits made to the SLIC data with the fixed inverse slope of -3 in Fig. 8(b) shows that the revised D curves based on 75 % and 95 % confidence levels fall closer and upon the mean-2SD curve obtained from the SLIC data. It is important to note that since the data points from the completed tests in the SLIC project are associated with the number of cycles to failure of $N < 5 \times 10^6$, the revised S-N design curves could be generated only for the first part of the bi-linear log–log curve with $N \leq 10^7$ where the recommended slope is given as m = -3 in DNV-RP-C203 standard [3]. Further long-term tests on large thickness specimens need to be conducted in future work to compare the SMF values for the second part of the bi-linear log–log curve with the slope of m = -5, to the ones obtained from the present study on the first part of the curve with the inverse slope of m = -3. It is also worth highlighting that in the generation of the revised design curve according to the DNV approach, the original fixed inverse slopes recommended in DNV-RP-C203 are employed in the analysis. This shows a lack of flexibility in this approach, limiting its use to slight updates to the curve while maintaining the same level of unquantified conservatism, in particular where assessment of OWT monopiles is concerned.

7. Discussion

The presented results from the linear and Bayesian regression analyses show that the “mean-2SD” curves heavily depend on the exclusion/inclusion of the run outs and also the inverse slope of the S-N curve. Moreover, while the statistical approach recommended in DNV-RP-C203 standard allows for the variable inverse slope obtained from regression analysis being employed in the design of as-welded structures, the second approach detailed in DNV-RP-C203 proposes shifting the S-N design curve to the left using the same fixed inverse slopes as recommended in the standard. As stated in DNV-RP-C203, it is quite crucial to apply engineering judgment to obtain reliable and conservative design curves. In order to achieve this goal, there are a number of further considerations that need to be taken into account in conjunction with the results demonstrated above. These are presented and briefly discussed below.

7.1. Context of the learnings from the current work

It must be noted that the current study only concerns investigation of a relatively small number of experimental results from one population of data, and any learning from these should be considered within the context of the historic database and any new test data. However, the observations from the experimental data may allow justification of taking a different approach to the determination of the slope of the S-N curve, in particular for situations where the same level of constraint and structural residual stress may not be present that is currently assumed in recommended curves.

Furthermore, it must be added it is expected to be individual distinctions between subsets of data where fabrication and/or testing have been performed at different facilities. In the current approach the entire data set is treated as one population. This is not unlike the approach taken by current standards (such as BS7608) where data from various sources are pooled together in the analysis. This lacks a level of rigour in that different populations may have different weights (in terms of number of data points) and might therefore bias the overall results.

7.2. Inverse slope in the S-N curve

An important topic that needs to be considered for accurate interpretation of the data presented in this study is the origin of the fixed slope of S-N curves in international standards. While it has not been attempted here to produce an exhaustive literature review of the developments of the S-N curves over the past few decades, the historical small-scale fatigue test data on double V-grooved multi-pass butt welded steel specimens, which were originally employed in derivation of the S-N design curves, must be revisited. These data points are from the studies going as far back as the late 60s and the 70s conducted by various researchers (e.g. [20–22]), which were

available at the time when the initial versions of design curves were developed. In a study by Gurney and Maddox [23], an argument was made that the small-scale specimens do not represent the residual stress state in larger welded structures. Therefore, they made an engineering judgment to propose a procedure which involves rotation of the S-N curve in order to account for residual stresses in larger welded structures.

Moreover, an argument was built by Gurney and Maddox in [23] that in large-scale butt-welded structures crack propagation might occur due to the presence of pre-existing small defects in the weld region, hence they proposed to take the exponent in the Paris law equation as a conservative estimate of the inverse slope in the S-N curve for cases where crack initiation is negligible and instead fracture mechanics dominates the failure process. Using this argument, they demonstrated that the inverse slope of around −3, taken from the stress intensity factor exponent in fracture mechanics test data on butt-welded samples, was in good agreement with their proposed procedure of S-N curve rotation. The proposed procedure by Gurney and Maddox described in [23] resulted in introduction of the reduced inverse slope of m = -3 for $N \leq 10^7$ in the design standards including the D curve in DNV-RP-C203 [3].

The rotation of the S-N curve to a lower inverse slope of m = -3 was originally proposed to account for the detrimental effect of tensile residual stresses, which are absent in small-scale samples, on fatigue life of large-scale welded structures. However, the SLIC data show that in large thickness multi-pass butt-welded specimens the magnitudes of the inverse slope obtained from linear and Bayesian regression analyses (see Tables 1 and 2) are higher than the fixed value of m = -3 implemented in the current design curves. Assuming that the state of residual stresses in the thick as-welded SLIC samples was similar to the welds in monopiles, this observation suggests that sufficient level of welding residual stresses remained active during the early stages of fatigue life and subsequently redistributed under cyclic loading condition. Moreover, assuming that unlike other large braced structures such as jackets no additional long-range residual stresses are present in monopile girth welds, the SLIC test results describe the fatigue behaviour of monopile circumferential welds without the need to apply any correction on the inverse slope to account for additional sources residual stresses.

It has been explained in [23] that when crack-like defects are present near the outer surface of the welded joints, crack initiation would be negligible and instead the fracture mechanics approach can be employed to identify a lower limit value for the inverse slope of the S-N curve from the Paris law exponent. The fracture mechanics data set that is referred to in [23] suggests a value of around 3 for the Paris law exponent; however, the results obtained from fracture mechanics tests on S355 steel specimens extracted from monopile weldments suggest that this value is 3.97 for the heat affected zone (HAZ) and 3.30 for the base metal (BM) in air [14]. Although these relate to only one set of data points, the comparison is useful in that even for OWT monopile welds containing considerable yet acceptable fabrications flaws, where fatigue cracks starts to propagate from early stages of operational life in the HAZ region and penetrate into the BM due to the geometry of the double V-grooved butt-welded structure, the inverse slope of the S-N curve may be taken as the conservative value of −3.30 which is still above the value of −3 implemented in standards. The size of the data set is obviously an important factor and the example above is presented for illustration only.

7.3. Long-term fatigue behaviour

A review of the existing fatigue data on small-scale weld samples, such as the collection of fatigue data sets available in the open literature presented in [24], shows that the dominant majority of the existing data points for as-welded condition are available for $N < 5 \times 10^6$. The data points from completed tests on large thickness welded specimens from the SLIC project are also available for $N < 5 \times 10^6$ (see Fig. 3). This means that while there is sufficient population of data points available in relatively low cycle region, there is an essential need to experimentally evaluate the long-term fatigue behaviour of welded structures, particularly monopiles, in the high cycle region ($N > 10^7$). Knowing that the operational loading conditions in OWT monopile foundations results in relatively low stresses applied on the structure, the lack of sufficient number of test data in the high cycle region can introduce significant uncertainty in the long-term fatigue behaviour of the structure. Although the current best practice of employing DFFs (typically 3 or 10) is believed to provide a good target level of fatigue reliability, it should be noted that these factors are derived based on the current two slope S-N curves in standards, and the assumed loading in these is a legacy Oil & Gas loading on fixed structures (typically 5–10 million load cycles per annum for a fixed structure in the North Sea, for a detail with a 20-year design life). Loading conditions on OWT monopiles are different, and the number of load cycles in a year are notably larger. Therefore, there is not sufficient confidence in these DFFs for the ongoing needs towards life extension of offshore monopile structures beyond the initial design life. It is worth noting that with the advancement in fatigue testing techniques in recent years, there are a number of methods available which allow accelerated fatigue testing being conducted with high frequencies. So there is need to explore the long-term fatigue behaviour of welded joints using these methods to inform decisions regarding long-term integrity assessment of offshore welded structures for life extension purposes.

It has been shown in the literature that the application of cyclic loads on welded structures can redistribute and relax the locked-in residual stresses (see e.g. [10–12]). This relaxation would be more severe when high stresses are applied on the structure, such as the hammering loads during piling. On the other hand, the residual stress relaxation would occur with a lower pace at low stress levels. This means that under operational loading conditions, the residual stresses remain in OWT monopiles for longer periods of time. Therefore, in evaluation of residual stress effects on fatigue life different considerations must be made for the long-term (i.e. low stress range) fatigue behaviour with long-lasting influence of residual stresses compared to short-term (i.e. high stress range) fatigue behaviour. This may need to be considered in the study of stress sequencing in variable amplitude fatigue within the context of Miner's rule, with variable amplitude fatigue being the key driver of fatigue damage in the high cycle region.

7.4. Other considerations

As shown earlier in Eq. (3), there is an empirical formulation available in DNV-RP-C203 [3] to apply thickness correction to S-N

design curves. A similar formula can be also found in BS 7608 [7]. A review of the fatigue test data available in the literature for different thicknesses show that there are insufficient data points available for welded specimens with large thicknesses. The collated literature data presented in [24] shows that the majority of the fatigue tests on butt-welded samples were conducted on thicknesses of $t \leq 22$ mm with limited number of data points available at $t = 32$ mm and $t = 38$ mm. The limited data available on thick welded specimens poses a question around the accuracy of the thickness correction function specified in standards for significantly larger thicknesses which are implemented in design of OWT monopile foundations. This implies that more tests need to be conducted on thicker welded structures to evaluate the upper limit for validity of the thickness correction factors specified in international standards.

Moreover, the entire analysis presented in this study is focused on the fatigue behaviour in air; however, further studies need to be conducted in future work to evaluate the short-term and long-term fatigue behaviour of welded structures in seawater environment with cathodic protection and free-corrosion condition, and examine the accuracy of the life reduction factors specified in standards.

Furthermore, it has been mentioned in standards that the fatigue tests performed in laboratories, based on which the S-N design curves are generated, are conducted under constant amplitude cyclic loading conditions. When the maximum and minimum loads are kept constant throughout the test, a fatigue endurance limit is expected to appear in the high cycle region which would make it difficult to evaluate the long-term fatigue behaviour of real-life structures. In reality, the offshore welded structures such as OWT monopile foundations, operate under variable amplitude cyclic loading conditions. Although the inverse slope of $m = -5$ has been proposed in DNV-RP-C203 [3] for the high cycle region (with $N > 10^7$) of class D design curve, further investigations must be carried out in future work to reduce the uncertainties involved in evaluation of the long-term fatigue behaviour of as-welded structures under variable amplitude loading conditions.

Last but not least, while the main focus of the argument raised in the present study is to evaluate the accuracy of artificially fixed inverse slope of -3 for application in offshore wind monopiles, a quantified analysis of the knowledge gap regarding the confidence bounds for the inverse slope will need be addressed in a subsequent investigation by considering a sufficiently large data set in conjunction with the manufacturing quality (i.e. weld toe angle, weld defects, etc) of the welded samples.

8. Conclusions

This study presents a re-evaluation of the fatigue design curves for as-welded OWT monopile foundations. The large thickness fatigue test data from the SLIC project were analysed using the linear and Bayesian regression analysis methods based on variable (i.e. unfixed) and fixed inverse slope assumptions. A review of the original source of the inverse slope of $m = -3$ showed that this value is based on an old correction approach which aimed to account for residual stresses in larger welded structures. While this inverse slope can be an acceptable basis for the design of braced structures with long-range residual stresses, the results from the SLIC project show that the magnitude of the inverse slope in monopile weldments is higher than -3 and can range between $-3.5 \leq m \leq -3.36$ depending on the regression model employed in the analysis and also censoring or censoring the data points using the Bayesian regression analysis method. Comparison of the regression analysis results with the thickness corrected D curve from DNV-RP-C203 shows that the fixed slope of $m = -3$ implemented in the thickness corrected D curve results in unconservative and over-conservative design of OWT monopiles in the high stress and low stress regions, accordingly. The $s_{\log N}$ values obtained from the linear and Bayesian regression analyses on completed SLIC test data are found to be close to, but slightly higher than, $s_{\log N} = 0.2$ which is specified in DNV-RP-C203. Last but not least, while the proposed procedure based on the statistical approach in DNV-RP-C203 leads to more conservative revised curves compared to mean-2SD curve obtained from the SLIC data, the alternative SMF approach only shifts the existing D curve to the left by forcing a fixed inverse slope of -3 without allowing the m value to be revised based on the large thickness test data. Other areas of research that need to be considered in future work for fatigue design enhancement of monopiles include investigation of the long-term fatigue behaviour, variable amplitude fatigue loading condition, thickness effects and environmental effects on the fatigue behaviour of large-scale structures.

CRediT authorship contribution statement

Ali Mehmanparast: Conceptualization, Investigation, Methodology, Validation, Formal analysis, Writing – original draft. **Amir Chahardehi:** Conceptualization, Investigation, Methodology, Validation, Writing – review & editing. **Feargal Brennan:** Validation, Writing – review & editing. **Mark Manzocchi:** Methodology, Formal analysis, Validation, Writing – review & editing.

Declaration of competing interest

The authors declare that they have no known competing financial interests or personal relationships that could have appeared to influence the work reported in this paper.

Data availability

Data will be made available on request.

Acknowledgments

The authors would like to thank Dariusz Eichler from Vattenfall and Marc Seidel from Siemens Gamesa Renewable Energy for constructive discussions throughout this study. This work was supported by the Supergen ORE Hub Flexible Funding under grant number EP/S000747/1 from the UK Engineering and Physical Sciences Research Council (EPSRC). The financial support from Kent for Amir Chahardehi and Mark Manzocchi to work on this study is greatly acknowledged.

Appendix A:. SLIC as-welded fatigue test data

See Table A1.

Table A1
SLIC fatigue test results on as-welded specimens [16].

Test Number	Stress range (MPa)	Cycles	Status
1	129.92	2,247,933	Complete
2	147.83	767,916	Complete
3	207.17	282,663	Complete
4	273.94	150,111	Complete
5	178.54	1,076,794	Complete
6	181.28	5,360,000	Suspended
7	221.63	305,111	Complete
8	304.93	51,321	Complete
9	199.01	153,434	Complete
10	150.86	471,655	Complete
11	263.57	103,228	Complete
12	180.78	327,000	Complete
13	186.50	269,429	Complete
14	155.12	400,000	Complete
15	127.96	550,000	Complete
16	99.68	4,860,000	Complete
17	233.37	128,284	Complete
18	129.32	3,137,400	Complete
19	208.93	263,303	Complete
20	102.63	1,892,200	Complete
21	174.16	338,335	Complete
22	151.52	415,000	Complete
23	225.79	152,700	Complete
24	159.01	589,800	Complete
25	102.96	1,550,000	Complete
26	130.94	1,100,000	Complete
27	204.39	368,260	Complete
28	223.21	265,878	Complete
29	99.03	6,199,999	Suspended
30	125.98	3,174,685	Complete
31	128.47	1,196,200	Complete

Appendix B:. Details of Bayesian regression analysis

See Figs. B1-B4.

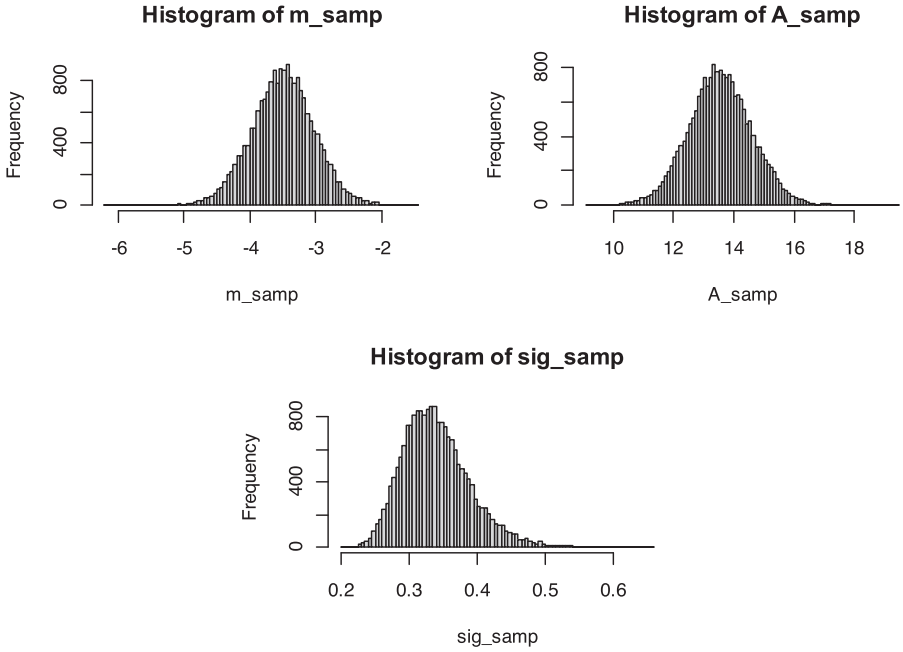

Fig. B1. Histograms of Markov chain Monte Carlo samples of regression parameters for censored data (i.e. including run outs) and variable inverse slope.

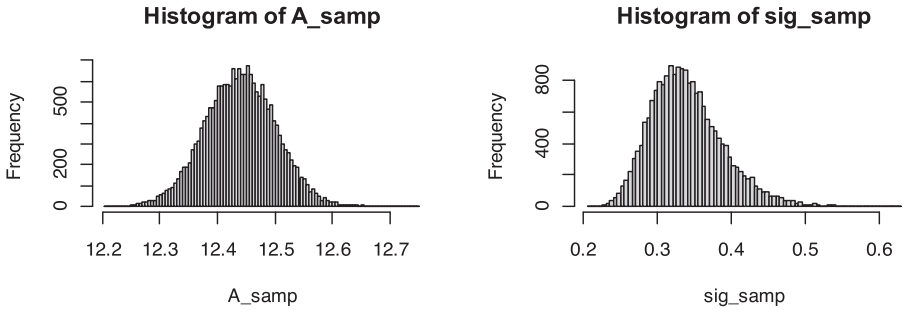

Fig. B2. Histograms of Markov chain Monte Carlo samples of regression parameters for censored data (i.e. including run outs) and fixed inverse slope of m = -3.

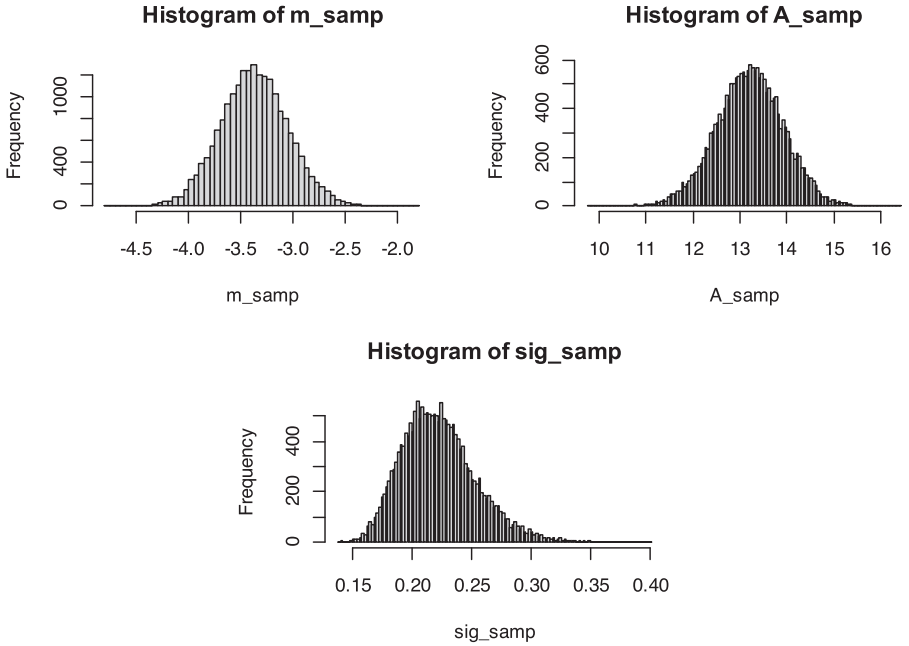

Fig. B3. Histograms of Markov chain Monte Carlo samples of regression parameters for uncensored data (i.e. excluding run outs) and variable inverse slope.

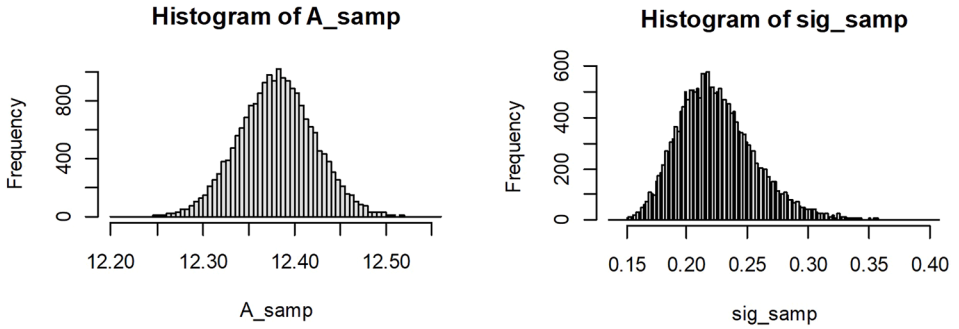

Fig. B4. Histograms of Markov chain Monte Carlo samples of regression parameters for uncensored data (i.e. excluding run outs) and fixed inverse slope of m = -3.

See Tables B1-B4

Table B1
Bayesian regression analysis results for censored SLIC data (i.e. including run outs) with variable inverse slope.

	Mean	2.5	25	50	75	97.5
A	13.56	11.44	12.86	13.56	14.24	15.65
m	−3.50	−4.44	−3.81	−3.50	−3.19	−2.56
$s_{\log N}$	0.34	0.26	0.30	0.34	0.37	0.45

Table B2
Bayesian regression analysis results for censored SLIC data (i.e. including run outs) with fixed inverse slope.

	Mean	2.5	25	50	75	97.5
A	12.44	12.32	12.40	12.44	12.48	12.56
m	−3.00	−3.00	−3.00	−3.00	−3.00	−3.00
$s_{\log N}$	0.34	0.26	0.30	0.34	0.37	0.45

Table B3
Bayesian regression analysis results for uncensored SLIC data (i.e. excluding run outs) with variable inverse slope.

	Mean	2.5	25	50	75	97.5
A	13.21	11.75	12.72	13.21	13.67	14.60
m	−3.36	−3.99	−3.58	−3.36	−3.15	−2.72
$s_{\log N}$	0.22	0.17	0.20	0.22	0.24	0.30

Table B4
Bayesian regression analysis results for uncensored SLIC data (i.e. excluding run outs) with fixed inverse slope.

	Mean	2.5	25	50	75	97.5
A	12.38	12.30	12.35	12.38	12.41	12.46
m	−3.00	−3.00	−3.00	−3.00	−3.00	−3.00
$s_{\log N}$	0.22	0.17	0.20	0.22	0.24	0.30

References

[1] I. Lotsberg, Assessment of the size effect for use in design standards for fatigue analysis, Int. J. Fatigue 66 (2014) 86–100.
[2] DNV-ST-0126: Support structures for wind turbines, Det Norske Veritas, Edition 2021-12.
[3] DNV-RP-C203: Fatigue design of offshore steel structures, Det Norske Veritas, Edition 2021-09.
[4] DNV's legal disclaimer: https://www.dnvgl.com/rules-standards/legal-disclaimer.html (accessed on 06/11/2023).
[5] MT Højgaard A/S (Respondent) v E.On Climate & Renewables UK Robin Rigg East Limited and another (Appellants), 2017, UKSC 59 (taken from: https://www.supremecourt.uk/cases/uksc-2015-0115.html, accessed on 06/11/2023).
[6] API Recommended Practice 2A-WSD: Planning, designing, and constructing fixed offshore platforms—working stress design, American Petroleum Institute, Reaffirmed Edition 2020-09.
[7] BS 7608: Guide to fatigue design and assessment of steel products, British Standards Institution, Edition 2014+A1:2015.
[8] Eurocode 3: Design of steel structures. European Standard, Edition EN 1993-1-9.
[9] A. Jacob, J. Oliveira, A. Mehmanparast, F. Hosseinzadeh, J. Kelleher, F. Berto, Residual stress measurements in offshore wind monopile weldments using neutron diffraction technique and contour method, Theor. Appl. Fract. Mech. 96 (2018) 418–427.
[10] X.F. Xie, W. Jiang, Y. Luo, S. Xu, J.M. Gong, S.T. Tu, A model to predict the relaxation of weld residual stress by cyclic load: Experimental and finite element modeling, Int. J. Fatigue 95 (2017) 293–301.
[11] L. Wang, X. Qian, Welding residual stresses and their relaxation under cyclic loading in welded S550 steel plates, Int. J. Fatigue 162 (2022) 106992.
[12] Q. Wang, X. Liu, Z. Yan, Z. Dong, D. Yan, On the mechanism of residual stresses relaxation in welded joints under cyclic loading, Int. J. Fatigue 105 (2017) 43–59.
[13] O. Adedipe, F. Brennan, A. Mehmanparast, A. Kolios, I. Tavares, Corrosion fatigue crack growth mechanisms in offshore monopile steel weldments, Fatigue Fract. Eng. Mater. Struct. 40 (11) (2017) 1868–1881.
[14] A. Mehmanparast, F. Brennan, I. Tavares, Fatigue crack growth rates for offshore wind monopile weldments in air and seawater: SLIC inter-laboratory test results, Mater. Des. 114 (2017) 494–504.
[15] A. Mehmanparast, J. Taylor, F. Brennan, I. Tavares, Experimental investigation of mechanical and fracture properties of offshore wind monopile weldments: SLIC interlaboratory test results, Fatigue Fract. Eng. Mater. Struct. 41 (12) (2018) 2485–2501.
[16] Marine Data Exchange, 2019, Structural Lifecycle Industry Collaboration (SLIC), S-N Curves and Guidance for Fatigue Assessment of Butt Welded Thick Steel Plates based on Large Scale Tests (https://www.marinedataexchange.co.uk/details/2115/packages accessed 06/11/2023).
[17] ASTM E739-10: Standard Practice for Statistical Analysis of Linear or Linearized Stress-Life (SN) and Strain-Life (ε-N) Fatigue Data. American Society for Testing and Materials, Edition 10(2015).
[18] BS EN ISO12107, Metallic materials - fatigue testing - statistical planning and analysis of data, British Standards Institution, Edition (2003).
[19] A.F. Desmond, On the relationship between two fatigue-life models, IEEE Trans. Reliab. 35 (2) (1986) 167–169.
[20] I. Yamaguchi, Y. Terada, A. Nitta, On the fatigue strength of steels for ship structures, IIW Doct. (1966). XIII-425-1966.
[21] H.S. Reemsnyder, Some significant parameters in the fatigue properties of weld joints, Weld. Res. 34 (5) (1969).
[22] J.D. Harrison, Fatigue tests on large butt welds. CIRIA Report 19. Feb 1970.
[23] T.R. Gurney, S. Maddox, A re-analysis of fatigue data for welded joints in steel, Weld. Res. Int. 3 (4) (1973).
[24] M. Feldmann, H. Bartsch, T. Ummenhofer, B. Seyfried, U. Kuhlmann, K. Drebenstedt, Neubewertung und Erweiterung des Kerbfallkataloges nach Eurocode 3 für eine zukunftsfähige Auslegung hochbeanspruchter Stahlkonstruktionen. AiF-DASt-FOSTA research project IGF-No. 19178N, final report, 2020.